Improving the Accuracy in Predicting Water Vapor Attenuation at Millimeter-wave for Earth-space Applications

Lorenzo Luini, *Member, IEEE* and Carlo Riva, *Member, IEEE*

***Abstract*— This contribution focuses on improving the accuracy of the simplified method currently recommended by the ITU-R for the prediction of water vapor attenuation at millimeter-wave on Earth-space links (Annex 2, paragraph 2.3 of recommendation ITU-R P.676-10), which receives as input only the local integrated water vapor content *V*. The main improvement to such model originates from taking into account the dependence of the water vapor mass absorption coefficient a_V on the reference site altitude, which is investigated by taking advantage of an extensive set of radiosonde observations (RAOBS) collected in several sites worldwide and characterized by high accuracy and reliability. Tested against attenuation estimates obtained from mass absorption models coupled with the mentioned RAOBS data, the model's prediction accuracy turns out to improve significantly with respect to the current recommendation and to be less dependent both on the operational frequency (20-100 GHz range) and on the considered site.**

***Index Terms*— Electromagnetic wave propagation, water vapor attenuation, atmospheric effects**

I. Introduction

NOWADAYS satellite communication (SatCom) systems are gradually shifting from simply broadcasting television channels to the provision of more complex interactive services (e.g. Internet via satellite), which address an always increasing number of users [1]. This is made possible in first place by the exploitation of higher frequency bands (e.g. Ka, but also Q and V in the near future), which, on the other hand, are associated to a strong increase in the atmospheric impairments [1],[2]. Though rain always plays the prevalent role in the millimeter-wave range, it is of key importance to make use of accurate models for the prediction of the impact of any constituent interacting with electromagnetic waves, i.e. also clouds, water vapor and oxygen [3]. In fact, as frequency increases, it is more and more cumbersome to guarantee high levels of system availability, such that even small differences in the power margin devoted to counteracting atmospheric impairments might have a determinant role on the link quality. Moreover, although gases typically provide a lower contribution to total attenuation if compared to clouds and hydrometeors – except for frequencies close to absorption peaks (e.g. around 22 GHz for water vapor and 60 GHz for oxygen), they are always present in the atmosphere: for some applications involving very low elevation angles (e.g. links from ground to Unmanned Aerial Vehicles or to Low Earth Orbit satellites [4]), even in clear sky conditions, the path attenuation might be in the order of several dBs (especially in tropical/equatorial sites) [5], such that any improvement in the model's prediction accuracy could be of key importance to correctly estimate the link performance.

The most accurate and acknowledged model for the prediction of water vapor attenuation A_V is included in Annex 1 of recommendation ITU-R P.676-10, which requires as input vertical profiles of pressure (P), temperature (T) and relative humidity (RH) to take into due account the dependence of the specific attenuation along the profile on pressure and temperature [6]. As such kind of data is not easily retrievable worldwide, the same recommendation defines a simplified approach in Annex 2 (paragraph 2.3) for the prediction of A_V (henceforth referred to as "simplified ITU-R model" in this work), which receives as input only the integrated water vapor content, V, rather than the full atmospheric profiles.

This contribution focuses on enhancing the accuracy of such simplified model in the 20-100 GHz frequency range. The main improvement originates from taking into account the dependence of the water vapor mass absorption coefficient a_V (lying at the basis of the said methodology) on the reference site altitude, which is investigated by taking advantage of an extensive set of radiosonde observations (RAOBS) collected in 24 sites worldwide and characterized by high accuracy and reliability.

The remainder of the paper is organized as follows: Section II presents the RAOBS dataset, while the central part of this work lies in Section III, dealing with the simplified ITU-R model and with its refinement; Section IV includes tests on the

Manuscript received XXXX.

Lorenzo Luini and Carlo Riva are with the Dipartimento di Elettronica, Informazione e Bioingegneria, Politecnico di Milano, Piazza Leonardo da Vinci, 35, 20133, Milano, Italy, and with the Istituto di Elettronica e di Ingegneria dell'Informazione e delle Telecomunicazioni (IEIIT), CNR, Milano, Italy (e-mail: lorenzo.luini@polimi.it).

This work was supported in part by the Air Force Office of Scientific Research, Air Force Material Command, USAF, under Grant FA8655-13-1-3081.

accuracy of the original and enhanced simplified ITU-R models and Section V draws some conclusions.

II. The Radiosonde Observation Dataset

Radiosonde observations (RAOBS) are of key importance primarily for atmospheric sciences (for example, together with other sensors, they contribute to produce the boundary values to run meteorological forecasts using Limited Area Models), but are also of great usefulness for electromagnetic wave propagation, as they provide high-resolution key information on the state of the atmosphere, from which, in turn, the impact of water vapor and oxygen on millimeter waves can be accurately estimated [7]. In this work, we make use of an extensive set of RAOBS data characterized by worldwide coverage, long measurement duration and, most importantly, high accuracy and reliability.

The FERAS (FUB-ESA Radiosonde, being FUB the acronym for Fondazione Ugo Bordoni) radiosounding dataset was assembled by the European Space Agency (ESA), starting from an NCAR (National Center for Atmospheric Research) database. Specifically, it consists of vertical profiles of pressure, temperature and relative humidity, collected routinely twice a day (0 and 12 Coordinated Universal Time UTC) for ten years (1980-1989) in non-rainy condition in 24 sites spread across different countries: Table I summarizes the geographical coordinates and the altitude of the sites where RAOBS data were collected, showing coverage of different climates, e.g. from cold in Finland, to Mediterranean in Italy or to equatorial in Singapore.

TABLE I. Geographical coordinates and altitude of the sites where RAOBS data were collected.

Station name	Country code	Latitude (° N)	Longitude (° E)	Altitude (m a.m.s.l.)
Sodankyla	FI	67.22	26.39	178
Jokionen	FI	60.49	23.30	103
Stornoway	UK	58.13	353.41	14
Hemsby	UK	52.41	1.41	13
De Bilt	NL	52.06	5.11	2
Uccle	BX	50.48	4.21	104
Lyon	FR	45.44	5.05	240
Berlin	DE	52.29	13.25	46
Wien	OS	48.15	16.22	200
Milan	IT	45.26	9.17	107
Brindisi	IT	40.39	17.57	7
Trapani	IT	37.55	12.30	5
Cagliari	IT	39.15	9.03	4
Moscow	RUS	55.45	37.34	184
Tabuk	SD	28.22	36.35	771
Delhi	IN	28.35	77.12	281
Hong Kong	CH	22.19	114.10	65
Singapore	SR	1.22	103.59	14
Dal-El-Beida	AL	36.43	3.15	25
Cape Town	ZA	-33.58	18.36	46
San Diego	US (CA)	32.49	242.52	124
Denver	US (CO)	39.45	255.08	1611
Mexico City	MX	19.26	260.55	2231
Lihue-On-Kauai	US (HI)	21.59	200.39	36

A detailed description of the FERAS database can be found in the final report of the COST 255 project [8], which also lists the guidelines according to which all RAOBS data were accurately validated. First, original NCAR quality control marks were taken into account, if present, and, afterwards, plausibility and inconsistency checks were applied. For example: the validity range of ground pressure was set to 700-1100 hPa; RAOBS levels corresponding to inversions of pressure or height values were discarded; the validity range of temperature and dew point temperature was set to 183-333 K for the whole profile. Finally, after this pre-processing, outliers of the time series of integrated parameters such as the total water vapor content were identified and removed.

III. Water Vapor Attenuation

A. The reference methodology

For propagation applications in the mm-wave region, the attenuation due to water vapor can be accurately calculated using mass absorption models such as those proposed by Liebe *et al.* (MPM93) [9] and by Rosenkranz [10]. Such models take into account the microphysical effects of atmospheric components, including water vapor and oxygen. Both gases cause absorption of the electromagnetic energy due to resonant effects (rotation of the electric and magnetic dipoles) associated to specific peak frequencies (typically referred to as lines). As for water vapor, the specific attenuation depends on pressure, temperature and relative humidity. Specifically, *RH* is necessary to estimate the water vapor density v, which, in turn, is used together with P and T to calculate the water vapor specific attenuation α_V. As a result, the accurate calculation of α_V requires knowledge of the full P, T and *RH* (or v) vertical profiles, which, in turn, can typically be obtained by exploiting data collected by radiosondes. Given their accuracy, the estimates of gaseous attenuation at millimeter-wave provided by mass absorption models are typically considered as the reference against which prediction models are tested.

As an example, Fig. 1 shows *P-RH-T* vertical profiles measured by the radiosonde launched at Milano Linate airport (Fig. 1.a), Fig. 1.b) and Fig. 1.c), respectively), as well as the associated profile of water vapor specific attenuation at 22 GHz (Fig. 1.d)) estimated using the MPM93 model (the total path attenuation A_V is equal to 0.115 dB).

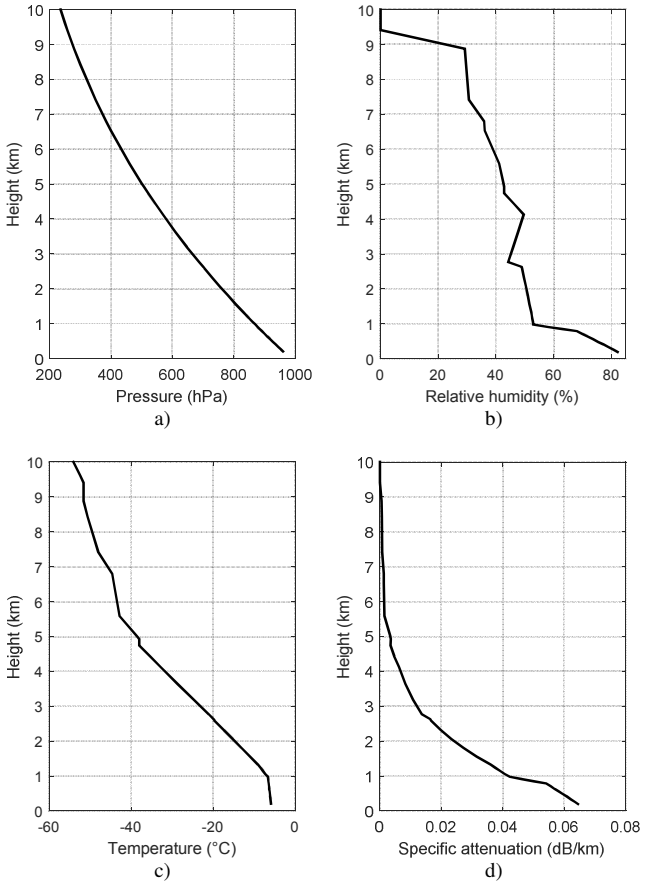

Fig. 1. Sample *P-RH-T* vertical profiles measured by the radiosonde launched at Milano Linate airport, and associated profile of water vapor specific attenuation at 22 GHz estimated using the MPM93 model [9].

B. The simplified ITU-R model

The methodology outlined in section III.A certainly guarantees a high accuracy in the prediction of water vapor attenuation (it lies at the basis of Annex 1 of the current recommendation ITU-R P.676-10 [6], where all the detailed calculations can be found), but, on the other hand, it is quite demanding in terms of inputs, as accurate high-resolution vertical profiles of the atmosphere can be hardly retrieved on global basis.

In order to address this issue, Salonen *et al.* proposed in [11] and [12] an approximate method to predict A_V, which, instead of making use of full vertical profiles of the atmosphere, receives as input V in mm, i.e. the water vapor content integrated along the path. Specifically, for a zenithal path:

$$A_V(f) = a_V(f_{ref}) \frac{\gamma_v(f, P_{ref}, v_{ref}, T_{ref})}{\gamma_v(f_{ref}, P_{ref}, v_{ref}, T_{ref})} V = \tilde{a}_V(f, V)\, V \qquad (1)$$

where:
f = frequency (GHz)
f_{ref} = 20.6 (GHz)
$a_V(f_{ref})$ = 0.0173 (dB/mm)
P_{ref} = 780 (hPa)
h_V = 4 (km)
$v_{ref} = V/h_V$ (g/m^3)
$T_{ref} = 14 \ln\left(0.22 v_{ref}\right) + 3$ (°C)
$\gamma_v(f, P, v, T)$ = specific attenuation in dB/km due to water vapor, calculated using equations (23a)-(23d) in recommendation ITU-R P.676-10 [6], as a function of frequency f, pressure P, water-vapour density v and temperature T.

The model above was conceived by Salonen *et al.* [11] by observing that the ratio between the specific water vapor attenuation γ_v at a reference frequency f_{ref} = 20.6 GHz and at the target frequency f is approximately equal to the ratio of the path attenuation $A_V(f_{ref})/A_V(f)$. Specifically, this occurs for a given reference pressure P_{ref} = 780 hPa [12]. It is also worth noticing that the simplified model introduced by Salonen *et al.* also depends on V through v_{ref}: instead of considering the full vertical trend of the water vapor content v with the height, v_{ref} is defined as a sort of "average value", obtained as the ratio between the integrated liquid water content V (mm) and the so-called water vapor scale height h_V (km), which regulates the decay of v with height h (v_G is the water vapor content at sea level expressed in g/m^3):

$$v(h) = v_G \exp(h/h_V) \qquad (2)$$

As a matter of fact, equation (1) offers a simplification to the calculation of A_V by proposing an approach based on the concept of mass absorption coefficient [7], which, in the specific case of (1) depends both on f and V (see the right end side of (1)). Finally, it is worth pointing out that, as already noticed in [11] (and confirmed later on in Section III.C), the model proposed by Salonen *et al.* relies on the observation that the variation of a_V from site to site is fairly limited and generally negligible for the electromagnetic wave propagation applications addressed in this work.

C. Model refinement

Though the methodology described in the previous section, adopted in recommendation ITU-R P.676-10 as well (Annex 2, paragraph 2.3), represents a simplified yet powerful approach to calculate water vapor attenuation, the accuracy of such a method might be restricted by the limited number of data used to tune its main parameters (e.g. the reference pressure P_{ref} and water vapor scale height h_V): indeed, to this aim, only one year of radiosonde observations (RAOBS) collected in five European sites were employed and the models' accuracy was evaluated against the same dataset only for some sample frequencies in the range 12 GHz $\le f \le$ 50 GHz [11].

In this section, we take advantage of the extensive RAOBS dataset presented in section II (24 sites spread worldwide, 10 years of measurements) to propose a refinement of the simplified approach described in Section III.B, as well as to more extensively test its accuracy on global basis.

The key idea at the basis of (1) is to embed into the water vapor mass absorption coefficient a_V the impact on A_V of the variation of T, P and RH with altitude. While the latter typically has a fairly irregular trend with height, as exemplified in Fig. 1, pressure and temperature are always associated to large negative gradients, such that, for instance, in the first 4 km, the value of P reduces to approximately half of its ground value, and T might decrease of 30 °C. This prompted us to investigate the possible variation of a_V as a function of the site altitude using the radiosonde database in Section II. Specifically, a_V was calculated as if the reference RAOBS site lay at a fictitious height a.m.s.l. (h_0), which means using as input to the MPM93 model RAOBS vertical profiles whose layers comprised between the sea level and h_0 are removed.

Fig. 2 shows, for some sample frequencies including the water vapor absorption peak at 22.235 GHz, the variation with h_0 of a_V^*, defined as the ratio between $a_V(h_0)$ and its value calculated close to the sea level, $a_V(0)$. The curves refer to the RAOBS station in Trapani, Italy, but very similar findings for a_V^* were obtained for all the other sites lying close to the average mean sea level, i.e. those allowing the full investigation of the a_V–h_0 relationship: according to Table I, De-Bilt (The Netherlands), Brindisi (Italy), Trapany (Italy) and Cagliari (Italy).

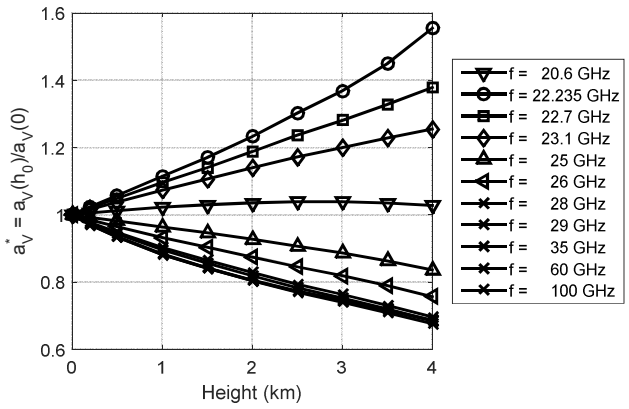

Fig. 2. Variation with h_0 of a_V^*, defined as the ratio between $a_V(h_0)$ and its value calculated close to the sea level, $a_V(0)$. Data from the RAOBS station in Trapani, Italy.

Results in Fig. 2 clearly indicate that, for the calculation of water vapor attenuation along the path, the change in a_V with h_0 is far from being negligible and that the rate of change varies with frequency: the most and less steep trends in the curves are associated to the water vapor absorption line at 22.235 GHz and to $f = 20.6$ GHz, respectively, while for $f \geq 28$ GHz, a_V^* is fairly independent of the frequency, at least up to 100 GHz.

Notwithstanding the marked differences shown in Fig. 2, the following power-law expression can be used to accurately model all the reported curves:

$$a_V^* = a\,h_0^b + c \quad \text{for} \quad h_0 \leq 4 \text{ km} \tag{3}$$

where a, b and c are fitting coefficients. Fig. 3 gives a hint of the high accuracy achieved by using (4) to fit the curves in Fig. 2 (f = 20, 22.235, 23.1 and 60 GHz). As indicated in equation (3), the validity of the proposed expression is limited to h_0 = 4 km: one the one side, most of the ground stations are likely to be installed at altitudes lower than 4 km and, on the other side, as also shown in Fig. 1.d), the impact of water vapor reduces considerably for $h_0 > 4$ km.

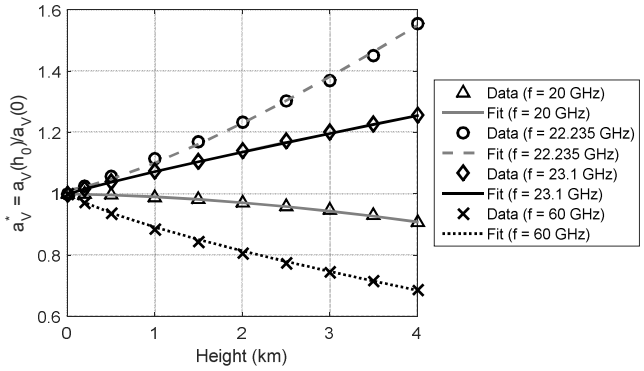

Fig. 3. Fitting the trend of a_V^* with h_0 using (4).

As a matter of fact, c can be set to 1, as it turns out to be practically independent of the frequency (it ranges between 0.999 and 1.007), while the dependence of a, b on f (the former is reported as an example in Fig. 4) can be accurately modeled using the following analytical formulations:

$$a = 0.205 \exp\left[-\left(\frac{f - 22.45}{3.034}\right)^2\right] - 0.113 \tag{4}$$

$$b = 8.741 \cdot 10^4 \exp(-0.587 f) + 312.2 f^{-2.38} + 0.723 \tag{5}$$

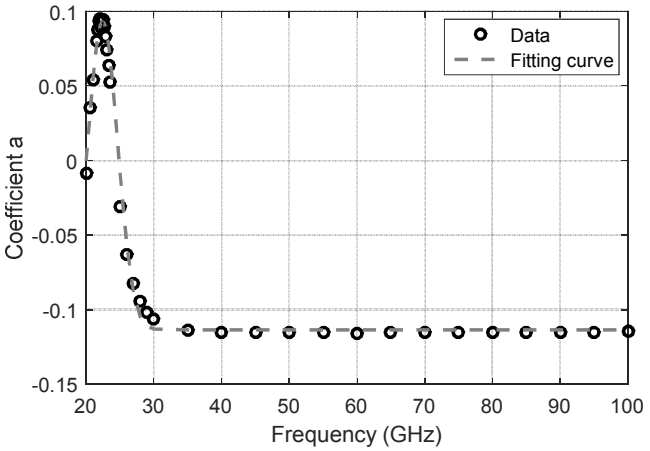

Fig. 4. Trend of coefficient a in (3) with frequency and its fitting expression in (4).

In the light of the dependence of a_V on h_0, and taking advantage of the availability of a more extensive RAOBS

dataset than that employed in [11], we have investigated the value of $a_V(f_{ref})$ in (1), i.e. the water vapor mass absorption coefficient at 20.6 GHz. This was done by using again the RAOBS data collected in the 24 sites. As an example, Fig. 5 shows the calculation of a_V(26 GHz) using data from Cagliari, Italy, which indicates a very high correlation coefficient of 0.998. Considering that the RAOBS sites listed in Table I lie at fairly different altitudes (as shown in the fifth column in Table I, h_0 ranges from 2 to 2231 m a.m.s.l.), all the a_V(26 GHz) values where first scaled to the same reference altitude, i.e. the average mean sea level, by using the relationships in equations (3) to (5):

$$a_V(f_{ref},0)=\frac{a_V(f_{ref},h_0)}{a(f_{ref})h_0^{b(f_{ref})}+c(f_{ref})} \quad (6)$$

As a matter of fact, the variation of $a_V(f_{ref},0)$ from site to site turns out to be practically negligible: indeed $\bar{a}_V(f_{ref},0)$, the mean value of $a_V(f_{ref},0)$, is 0.0176 and its standard deviation, normalized to $\bar{a}_V(f_{ref},0)$, is 1.5%. Thus, accounting also for the dependence of the water vapor mass absorption coefficient with altitude, equation (1) becomes:

$$A_V=0.0176\frac{\gamma_v(f,P_{ref},v_{ref},T_{ref})}{\gamma_v(f_{ref},P_{ref},v_{ref},T_{ref})}\left(a\,h_0^b+c\right)V=\tilde{a}_V(f,V,h_0)\,V \quad (7)$$

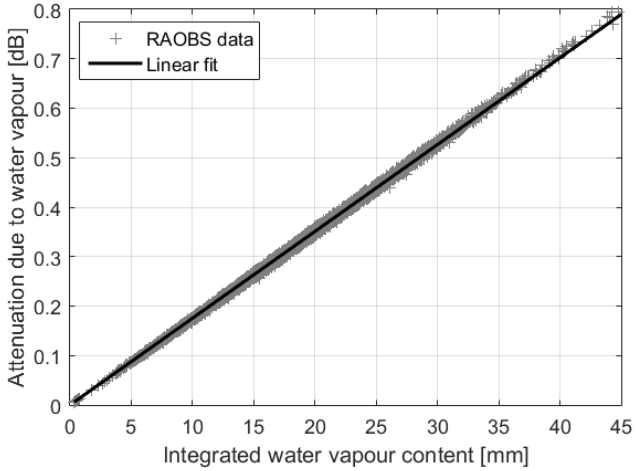

Fig. 5. Calculation of the mass absorption coefficient a_V at 20.6 GHz using the RAOBS data collected in Cagliari (MPM93 model).

The final elements investigated to refine the model in (1) are the reference pressure P_{ref} and average water vapor scale height h_V, respectively set to 780 hPa and 4 km in Annex 2 of recommendation ITU-R P.676-10 [6]. As a matter of fact, both values are effective parameters: in this work they were derived using an optimization procedure aiming at maximizing the agreement between A_V values calculated from the RAOBS dataset and the MPM93 model at frequencies in the range 20-100 GHz and path attenuation predictions obtained by applying (7) (V inputs extracted from RAOBS data as well). As a result, the following values were identified:

$$P_{ref}=880 \text{ hPa and } h_v=6.5 \text{ km} \quad (8)$$

As a final remark, only half of the 24 sites were selected (uniformly across the Globe) to derive P_{ref} and h_V in (8), while the remaining locations were employed only to perform independent tests on the model's prediction accuracy (see Section IV).

Fig. 6 and Fig. 7 give a hint of the dependence of $\tilde{a}_v$ on the integrated water vapor content V and on site altitude h_0: while the discrepancies in the former figure are fairly limited, the impact of h_0 is definitely significant.

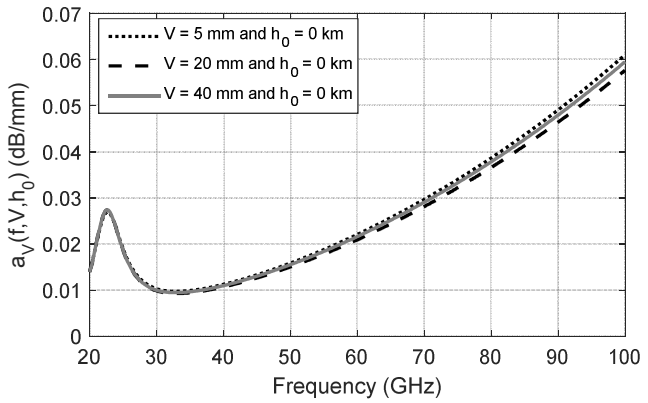

Fig. 6. Trend of the water vapor mass absorption coefficient with frequency, for different values of V and fixed h_0.

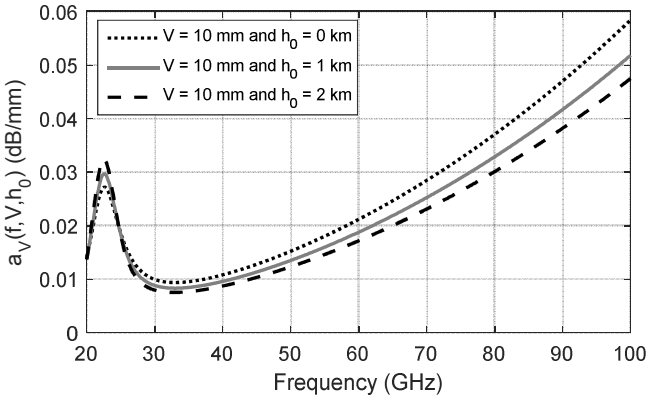

Fig. 7. Trend of the water vapor mass absorption coefficient with frequency, for different values of h_0 and fixed V.

IV. Accuracy Evaluation

The accuracy of the new expression proposed in (7) and (8) to estimate the water vapor attenuation along the path is assessed here against the complete set of RAOBS measurements introduced above. Fig. 8 shows an example of the zenithal water vapor attenuation statistics (Complementary Cumulative Distribution Function, CCDF) at 80 GHz calculated according to the MPM93 model using as input the whole *P-RH-T* profiles, the expression in (7) and the Annex 2

of ITU-R recommendation P.676-10, i.e. expression (1) (RAOBS data collected at Sodankyla, Finland).

The methods' prediction accuracy is quantified by the average (E) and root mean square (RMS) values (also reported in the legend of Fig. 8) of the following error figure (typically suggested by ITU-R in recommendation P.311-15 to compare tropospheric attenuation statistics [13]):

$$\varepsilon(P)=\begin{cases}100\left(\dfrac{A_V(P)}{10}\right)^{0.2}\ln\left(\dfrac{A_V^*(P)}{A_V(P)}\right) & A_V(P)<10\text{ dB}\\ 100\ln\left(\dfrac{A_V^*(P)}{A_V(P)}\right) & A_V(P)\geq 10\text{ dB}\end{cases} \quad (9)$$

where $A_V^*(P)$ and $A_V(P)$ are the water vapor attenuation values extracted from the estimated and reference attenuation statistics, respectively, relative to the same probability level $P \geq 0.05\%$.

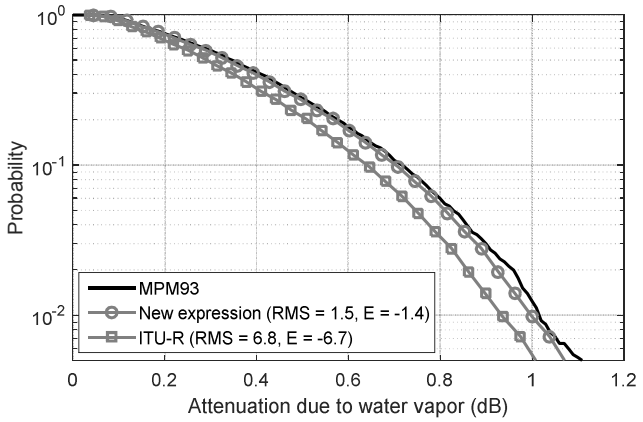

Fig. 8. Zenithal water vapor attenuation CCDF at 80 GHz calculated according to the exact method (black solid line), the new approximate expression in (7) (gray line with circles) and Annex 2 of recommendation ITU-R P.676-10 (gray line with squares) for the RAOBS data collected at Sodankyla, Finland.

Fig. 9 gives a summary of the accuracy of the method by reporting the mean E (ψ_E) and mean RMS (ψ_{RMS}) values as a function of frequency. Results indicate a very accurate prediction performance (overall ψ_{RMS} = 1.7), which is fairly constant with frequency. The ITU-R method shows a lower accuracy (overall ψ_{RMS} = 4.5) with a tendency to underestimation and a slight dependency on the frequency. Fig. 10 completes the prediction models' assessment by reporting ψ_{RMS} as a function of the site. Rather small variation of ψ_{RMS} are found from site to site for the new expression, which confirms the appropriateness of the site-independent assumption for $a_v(f)$. On the other hand, the simplified ITU-R method shows a more marked variability from site to site.

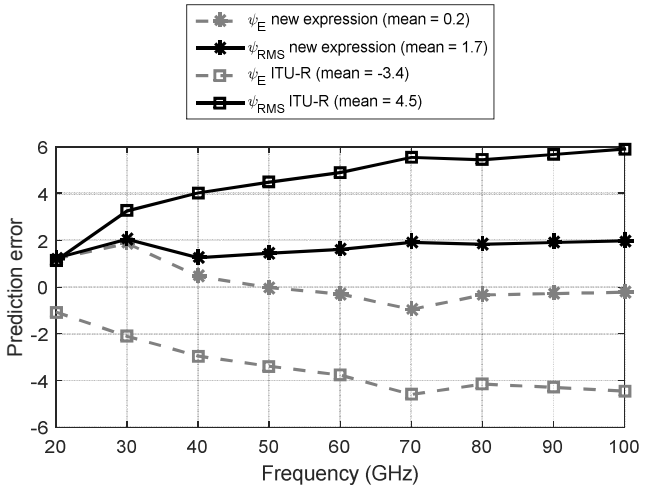

Fig. 9. Mean E (ψ_E) and mean RMS (ψ_{RMS}) as a function of frequency (average over all stations). *V* inputs extracted from the RAOBS dataset as well.

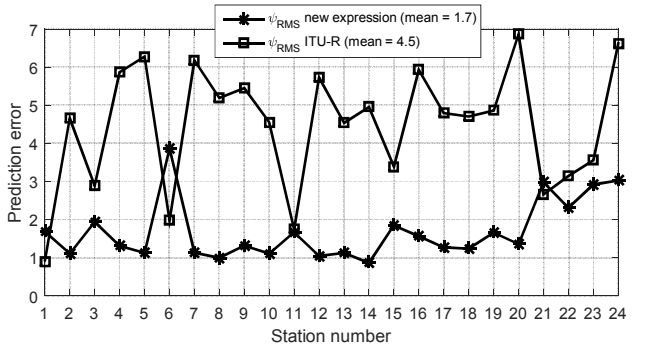

Fig. 10. Mean RMS (ψ_{RMS}) as a function of the RAOBS site (average over all frequencies). *V* inputs extracted from the RAOBS dataset as well.

While for the results shown in Fig. 9 and Fig. 10 the integrated water vapor values feeding the expressions in (1) and (7) are extracted from RAOBS data as well, the two models have been tested using as input *V* values coming from the ERA40 database included in recommendation ITU-R P.836-5 [14]: indeed, this is the dataset typically employed when applying the prediction model in Annex 2 of recommendation P.676-10. In this case ψ_E and ψ_{RMS} maintain trends similar to those reported in Fig. 9 and Fig. 10, but the overall scores slightly worsen as shown in Table II: as it turns out, overall, the new expression in (7) provides more accurate attenuation predictions than the model in ITU-R P.676-10. This true for $f \geq 40$ GHz, while for lower frequencies, the performance of the two models are basically the same. Although not shown here for brevity's sake, it is worth pointing out that, overall, *V* values extracted from recommendation ITU-R P.836-5 tend to overestimate the correspondent values measured by the radiosonde, which explains the performance decrease of the new expression in (7) with respect to the findings reported in Fig. 9 and Fig. 10.

TABLE II. OVERALL MODELS' PREDICTION ACCURACY: DIFFERENT SOURCES FOR THE INPUT QUANTITY V.

Input source for V	New expression		ITU-R P.676-10	
	ψ_E	ψ_{RMS}	ψ_E	ψ_{RMS}
V from RAOBS	0.2	1.7	-3.4	4.5
V from ITU-R P.836-5	3.4	5.7	-0.6	7.1

V. CONCLUSIONS

This contribution focuses on improving the accuracy of the simplified model currently recommended by the ITU-R (P.676-10, Annex 2) for the prediction of water vapor attenuation at millimeter-wave on Earth-space links, which receives as input only the information on the local integrated water vapor content V. Taking advantage of an extensive set of RAOBS ascents collected in several sites worldwide and characterized by high accuracy and reliability, the model's improvement is achieved mainly by investigating and modeling the dependence of the water vapor mass absorption coefficient a_V on the reference site altitude. In addition, two effective parameters, namely the "average" water vapor scale height h_V and the reference pressure level P_{ref}, are updated to 6.5 km and 880 hPa, respectively.

The improved model, tested against reference water vapor attenuation statistics obtained using the Liebe MPM93 model coupled with the mentioned RAOBS dataset, shows an excellent accuracy, both in terms of overall prediction error (average ψ_{RMS} for the current ITU-R model and its improved version equal to 4.5 and 1.7, considering all sites and all frequencies), as well as in terms of performance stability, which turns out to be almost independent of the frequency (20-100 GHz range) and of the considered site.

ACKNOWLEDGMENT

The authors would like to acknowledge Dr. Martellucci from the European Space Agency for the provision of FERAS radiosonde data.

REFERENCES

[1] N. Jeannin, L. Castanet, J. Radzik, M. Bousquet, B. G. Evans, P. T. Thompson, "Smart gateways for terabit/s satellite," *Int. J. Satellite Communications Networking*, 32(2): 93-106 (2014).

[2] R. Polonio, C. Riva, "ITALSAT propagation experiment at 18.7, 39.6 and 49.5 GHz at Spino D'Adda: three years of CPA statistics," *IEEE Transactions on Antennas and Propagation*, 46 (5), 631-635.

[3] C. Riva, C. Capsoni, L. Luini, M. Luccini, R. Nebuloni, A. Martellucci, "The Challenge of Using the W Band in Satellite Communication," *Int. J. Satell. Commun. Network*., 2014; 32:187–200.

[4] L. Luini, C. Capsoni, "Joint Effects of Clouds and Rain on Ka-Band Earth Observation Data Downlink Systems", pp. 1-5, *in Proc. EuCAP 2015*, 12-17 April 2015, Lisbon, Portugal.

[5] P. Bouchard, "Approximate Method for Estimating Gaseous Loss at Very Low Angles Along Paths of Finite Length and Earth-Space Paths," *IEEE Transactions on Antennas and Propagation*, 64 (2), 687-699.

[6] ITU-R recommendation P.676-10, "Attenuation by atmospheric gases," Geneva, Switzerland, 2013.

[7] L. Luini, C. Riva, C. Capsoni, A. Martellucci, "Attenuation in non rainy conditions at millimeter wavelengths: assessment of a procedure," *IEEE Transactions on Geoscience and Remote Sensing*, pp. 2150-2157, Vol. 45, Issue 7, July 2007.

[8] COST Action 255 Final Report, "Precipitation, Clouds and Other Related Non-Refractive Effects," J. P. V. Poiares Baptista, Ed. Noordwijk, The Netherlands: ESA Publication Division, ch. 3.2.

[9] H. J. Liebe, G. A. Hufford, M. G. Cotton, "Propagation modeling of moist air and suspended water/ice particles at frequencies below 1000 GHz," *in Proc. AGARD 52nd Spec. Meeting EM Wave Propag*.

[10] P. Rosenkranz, "Water vapor microwave continuum absorption: A comparison of measurements and models," *Radio Sci.*, vol. 33, no. 4, pp. 919–928, Jul./Aug 1998.

[11] E. Salonen, S. Karhu, P. Jokela, W. Zhang, S. Uppala, H. Aulamo, S. Sarkkula, "Study of propagation phenomena for low availabilities," Helsinki University of Technology Radio Laboratory and Finnish Meteorological Institute, Finland, Final Report for the European Space Agency under ESTEC contract 8025/88/NL/PR, Nov. 1990.

[12] E. Salonen, S. Karhu, S. Uppala, R. Hyvönen, "Study of improved propagation predictions," Helsinki University of Technology Radio Laboratory and Finnish Meteorological Institute, Finland, Final Report for the European Space Agency under ESTEC contract 9455/91/NL/LC(SC), Dec. 1994.

[13] ITU-R recommendation P.311-15, "Acquisition, presentation and analysis of data in studies of tropospheric propagation," Geneva, Switzerland, 2015.

[14] ITU-R recommendation P.836-5, "Water vapour: surface density and total columnar content," Geneva, Switzerland, 2013.